

An Experimental Investigation on the Dynamic Behavior of Step Motor Drives

Paolo Righettini, Roberto Strada, Alberto Oldani and Andrea Ginammi

Department of Design and Technologies, Faculty of Engineering, University of Bergamo, Dalmine 24044, Italy

Received: March 08, 2012 / Accepted: March 28, 2012 / Published: July 25, 2012.

Abstract: Step motors, compared to other drive systems, are low-cost and easy to use devices. However, despite these undeniable advantages, they are characterized by some critical running conditions, due to the loss of synchronization between the stator's magnetic field and the rotor. In order to theoretically investigate such a behavior, several complex mathematical models have been developed, which require several parameters to be defined. For most step motors, such parameters cannot be easily drawn from their data-sheets; on the contrary, in this paper the authors refer to a simplified electro-mechanical model where the most of the parameters are known from data-sheets. The dependence between electrical and mechanical quantities can be investigated by an experimental point of view. At this aim, a specific novel test rig has been designed and developed for either static or dynamic characteristics measurement of small size step motors. In particular, the test rig allow to measure rotor's angular position, motor's torque, currents flowing in the motor's phases. The paper ends with the report of the results of several experimental tests, carried-out on a small-size motor in different running conditions, and with some preliminary remarks on the basis of the measures analysis.

Key words: Step motor drives, experimental investigation, test-rig, dynamic behavior, electro-mechanical model.

1. Introduction

Step motors, compared to other drive systems, are low-cost and easy to use devices. For these reasons and thanks to their robustness and reliability they are widely used in several fields, mainly for small size automation. The typical incremental motion of a step motor allows to develop open-loop applications with high performances, cost effective and very simple to

Paolo Righettini, associate professor, research fields: mechatronic systems, kinematic and dynamic of redundant robots, automatic machines, multi-body systems, real-time systems, automatic control, electric actuators, pneumatic actuators, piezo-electric actuators, active vibration control.

Alberto Oldani, research assistant, research fields: mechatronic systems, kinematic and dynamic of vehicles, multi-body systems, real-time systems, HIL systems, automatic control.

Andrea Ginammi, research assistant, research fields: mechatronic systems, multi-body systems, kinematics and dynamics of parallel kinematic robots, haptic interfaces.

Corresponding author: Roberto Strada, assistant professor, research fields: mechatronic systems, electric actuators, modeling and simulation of fluid power systems and components (pneumatics, hydraulics), active vibration control. E-mail: roberto.strada@unibg.it.

implement, thanks to the lack of position and velocity transducers too.

However, despite these undeniable advantages, they are characterized by some critical running conditions, due to the loss of synchronization between the stator's magnetic field and the rotor [1]. In particular, the bad running conditions mainly depend on: (1) too high acceleration/deceleration of the law of motion imposed to the motor; (2) command frequency near to the motor's resonance frequency; (3) overcoming of the limits imposed by the pull-out curve.

In order to theoretically investigate such a behavior, several complex mathematical models have been developed, which require several parameters to be defined [2-5]. For most step motors such parameters cannot be easily drawn from their data-sheets; on the contrary, in this paper the authors refer to a simplified electro-mechanical model [1, 6-7] where the most of the parameters are known from data-sheets. The dependence between electrical and mechanical

quantities can be investigated by an experimental point of view.

At this aim, a specific novel test rig has been designed to investigate both the static and the dynamic characteristics of small size step motors, including their oscillatory behavior. In particular, the test bench allows to measure both mechanical quantities, such as torque and angular position, and electric quantities, such as phases currents.

The paper ends with the report of the results of several experimental tests carried-out on a small-size motor in different running conditions, and with some preliminary remarks based on the comparison between experimental and simulation results.

The paper is organized as follows: Section 2 describes the state of art concerning the static and dynamic characteristics of a step motor from a mainly mechanical point of view; in section 3, there is a detailed description of the test bench configuration and of the measurements that can be carried-out; section 4 reports the results of the experimental tests; in section 5, the measurement's results are discussed; in section 6, some conclusions are highlighted.

2. State of Art

Before to proceed, let's remember how the static and dynamic characteristics of a step motor can be described by a mainly mechanical point of view. A step motor is an incremental motion device; Fig. 1 shows a sketch of the running principle of a step motor (This kind of motor has one rotor poles couple and two stator salient poles: It hasn't practical application, it is just for explanation).

The rotor's motion is a consequence of the phases' supply switching along with the currents' flowing directions. In particular, starting from the initial condition where phase A is supplied by current i_A^+ (its direction considered as positive) the sequence $i_B^+, i_A^-, i_B^-, i_A^+$ causes one full revolution of the rotor. At each supply condition an ideal rotor's angular position corresponds. By supplying stator phases in suitable way (e.g., simultaneously), the rotor's ideal position

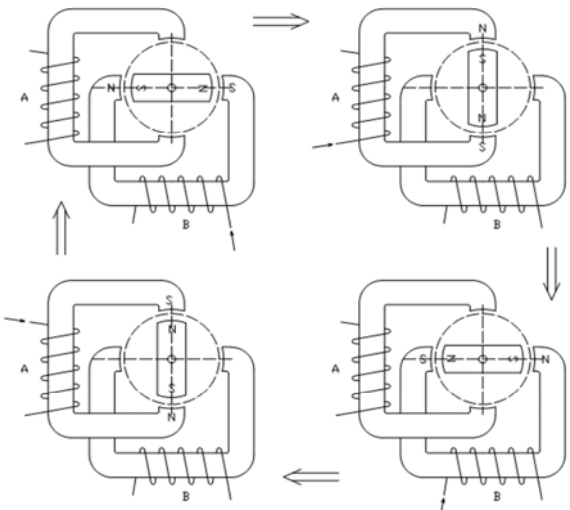


Fig. 1 Sketch of the running principle of a step motor.

could be intermediate; this is typical of a micro-step driving method.

Fig. 2 shows the static characteristic curves of a step motor for two different ideal rotor's equilibrium positions α_0 and α_1 . When a load torque is applied to the motor's shaft, the rotor changes its angular position; for the ideal position α_0 , the torque behaviour is described by the following equation:

$$T_m = T_H \sin \left[\frac{\pi}{2\alpha_p} (\alpha_0 - \alpha_m) \right] \quad (1)$$

where T_H is the holding torque, α_p is the step angle (1.8° for a 200 step/rev motor), α_0 is the ideal commanded rotor's position, α_m is the generic rotor's position.

When the applied load exceeds the holding torque, the motor "loses step", i.e., the rotor moves toward a new ideal equilibrium position.

The continuous running of a step motor is obtained by switching over the motor's phases at a frequency called command frequency (f_c).

At a given f_c value, the step motor keeps its angular speed constant independently of the load applied until a specific torque, called pull-out torque, is reached. When the load torque value reaches the pull-out torque's one, the motor loses synchronism and stops. Hence, a pull-out curve can be defined, its shape strongly depending on the electronic device used to drive the motor.

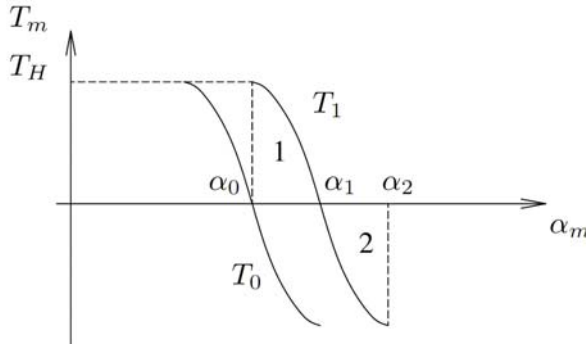


Fig. 2 Static characteristic.

Moreover, a step motor shows an oscillatory behavior when the phases switch over. As a matter of fact, with reference to Fig. 2, when the phase switches from ideal equilibrium position α_0 to ideal equilibrium position α_1 , it can be supposed that the static characteristic curve instantaneously changes from T_0 to T_1 , hence the rotor moves toward the new equilibrium position going beyond it, resulting in an oscillation around the new equilibrium position.

Hence, from a mechanical point of view, the step motor can be modeled as a 1 DOF vibrating system forced by the motion of the base (Fig. 3). Oscillations damping is mainly due to electromagnetic phenomena, while the stiffness is related to the static characteristic of the motor; the spring is non-linear, with a characteristic curve described by Eq. (1). As a matter of fact, the load torques acting on the step motor's shaft during its regular running condition, are the inertia torque, the damping torque and the motor's torque (Eq. (1)). Hence the system's dynamic behaviour can be described by the following mechanical equilibrium equation:

$$T_m = J\ddot{\alpha}_m + c\dot{\alpha}_m \quad (2)$$

where T_m is the motor's torque (Eq. (1)), J is the rotor's moment of inertia, c is the damping coefficient.

By linearizing and substituting Eq. (1) in Eq. (2), for a generic ideal rotor's angular position α , the following equation arises:

$$J\ddot{\alpha}_m + c\dot{\alpha}_m + T_H \frac{\pi}{2\alpha_p} \alpha_m = T_H \frac{\pi}{2\alpha_p} \alpha \quad (3)$$

from which the natural frequency of the system is found as

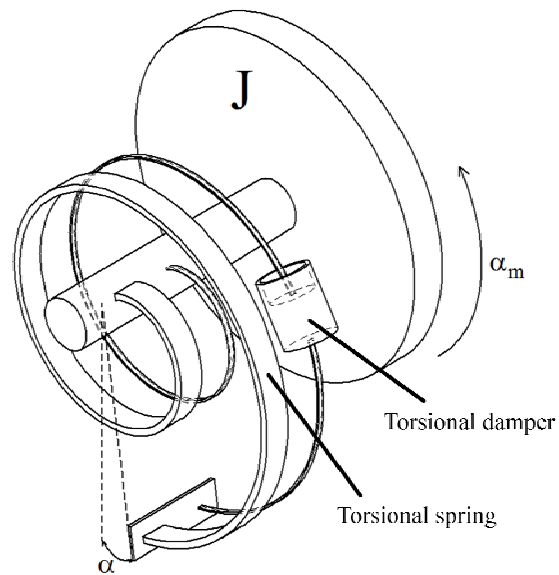


Fig. 3 Mechanical model of a step motor.

$$\omega_n = \sqrt{\frac{T_H}{J} \frac{\pi}{2\alpha_p}} \quad (4)$$

Hence, Eq. (3) is a linearized and mainly mechanical model of a step motor.

3. The Test Bench

Once summarized the main characteristics of a step motor, let's describe the configuration of the designed and developed test bench, whose conception is an evolution of a previous project [8].

Fig. 4 shows a sketch of the test bench's configuration. It is equipped with a position sensor, a torque sensor, current sensors and a device to apply the load to the motor. The test bench is designed for small size motors (max holding-torque 2 Nm); in particular the sizes that can be tested are 28, 35, 42, 50, 56 mm.

The test bench's frame is tubular; at its ends, the motor and the loading device are connected. Such a configuration creates a torque loop inside the frame, hence no ground reaction forces arise to guarantee the torque equilibrium.

In order to be able to connect the whole range of motor's sizes, the motor is connected to the tubular frame by means of two flanges, one independent by the type of motor tested (1), the other designed according to the motor's size (2) (Fig. 5).

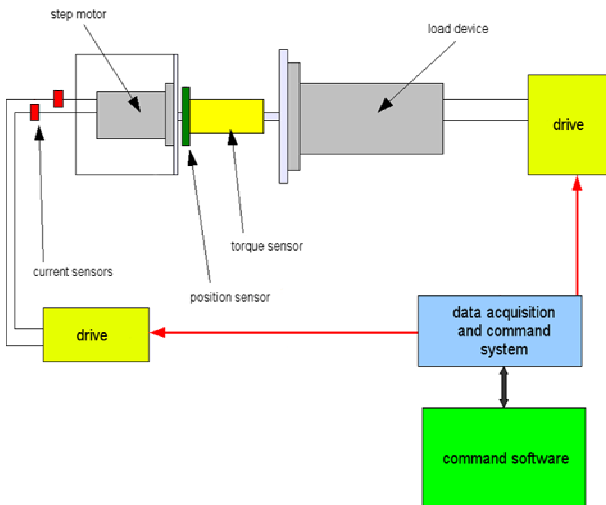


Fig. 4 Sketch of the test-bench's configuration.

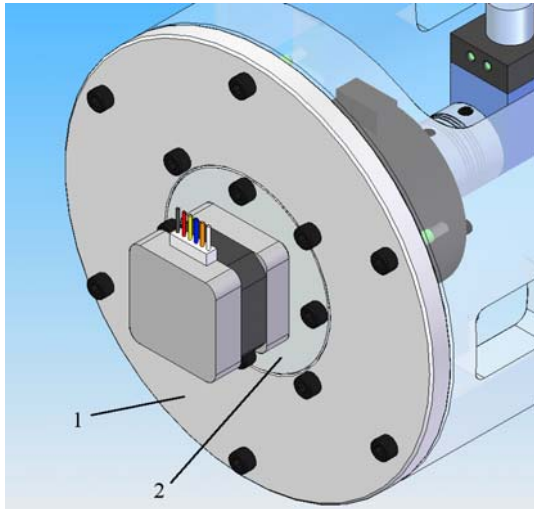


Fig. 5 Flanges for motors connections.

The aim of the bench is to execute experimental tests to measure and investigate the pull-out curve and the rotor's oscillatory behavior inside the step angle. Hence, the test bench has two different configurations: inside step and pull-out.

3.1 Inside Step Configuration

Figs. 6-7 show the inside-step configuration. The test bench is so configured when the goal is to investigate the oscillatory behavior of the step motor, within the step angle. In details, the system is composed as follows: The step motor (1) is connected with a high resolution encoder (3) by means of a rigid coupling (4) and an encoder coupling device (2).

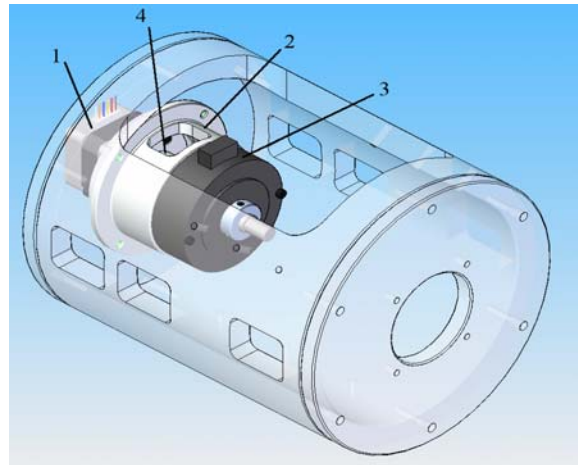


Fig. 6 Inside-step configuration.

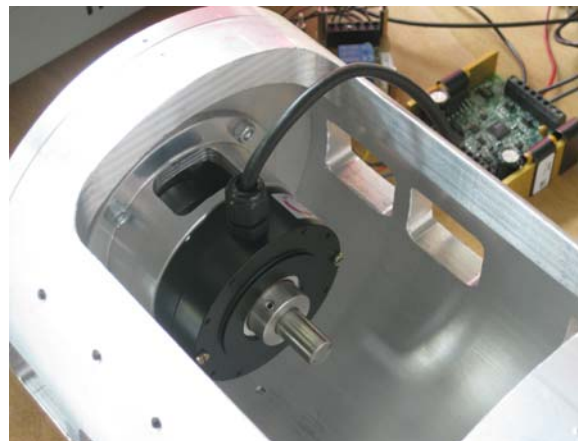


Fig. 7 Test bench in inside-step configuration.

The encoder has a resolution of 4,096 pulses/rev; the acquisition of its signal in X4 encoding leads to an angular resolution of 0.022° allowing to test the motor also at micro-step resolution. In addition to the angular position, the currents flowing in the two phases are measured too. The measurement has been performed by means of a LEM current transducer mod. HX05-P/SP2 (Fig. 8), which guarantees high frequency bandwidth (50 kHz).

3.2 Pull-Out Configuration

This configuration is devoted to the measurement of the pull-out curve; Figs. 9-10 respectively show the 3D model of the test bench, and the developed device. The configuration is as follows: (1) step motor under test; (2) encoder coupling device; (3) encoder; (4) torque sensor; (5) tubular frame; (6) brushless servomotor to generate

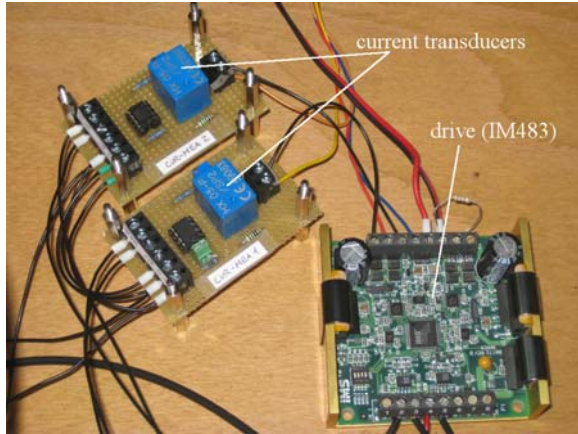


Fig. 8 Current transducers and motor's drive.

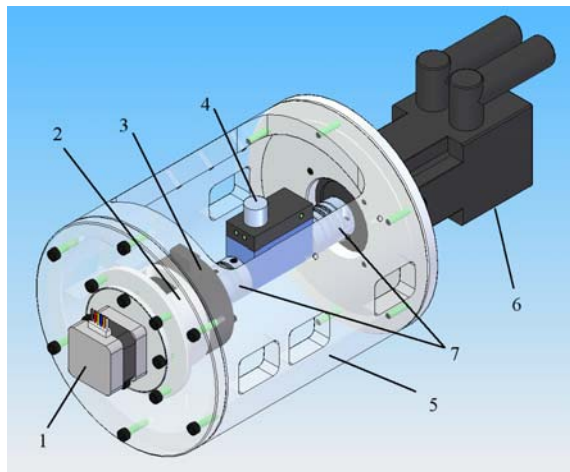


Fig. 9 Pull-out configuration.

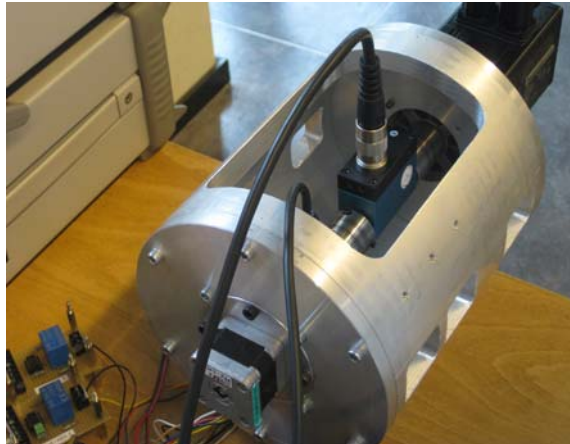


Fig. 10 Test bench in pull-out configuration.

the load torque; (7) torsionally rigid couplings. As shown in Figs. 9-10, a brushless servomotor is used as load generating device; this choice allows to test the motors also in the II and IV quadrants, i.e., when the load acts as a motor.

Moreover, according to the current set-point given to the brushless motor's drive, it is possible to simulate any kind of load. By giving to the servomotor's drive an increasing torque set point while the stator is in an equilibrium position, the static characteristic curve can be measured too.

In pull-out configuration it is not necessary to measure the angular position with high resolution, hence instead of the high resolution encoder, the angular position signal coming from the brushless motor's drive can be used.

4. Experimental Tests

Some preliminary tests have been performed with the designed and built test bench, mainly oriented to the investigation of the oscillatory behavior of the motor. Hence the reference configuration is the inside-step one. The tested motor is a Sanyo Denki mod 103-547-52500, fed by the driver IMS mod. IM483; motor's characteristics are summarized in Table 1.

The test has been carried out for different command frequencies, different motor's resolutions and different moments of inertia. In particular, two different resolutions have been considered, 400 and 800 steps/rev¹, and two different moments of inertia, $J_1 = 2.06 \times 10^{-5} \text{ kgm}^2$ and $J_2 = 1.45 \times 10^{-4} \text{ kgm}^2$. The first value is the total moment of inertia of the motor's shaft, of the rigid coupling between motor and encoder, and of the encoder's shaft. The second one is obtained by adding a pulley on the encoder's shaft.

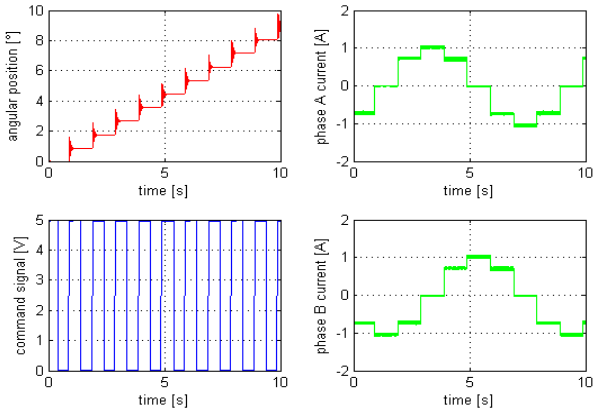
The following figures show the results of some tests highlighting some typical characteristics of step motors.

Fig. 11 shows a typical result of the test bench in inside-step configuration; the signals acquired and graphed are: the angular position of the motor's shaft, the command signal (a square wave with frequency equal to the desired f_c), and the currents flowing in the two motor's phases. The test of Fig. 11 has been carried-on with $f_c = 1 \text{ Hz}$, $n_p = 400 \text{ steps/rev}$, $J = J_1$. It

¹The motor hasn't been tested in full step configuration (200 steps/rev) because the minimum resolution allowed by the used drive (IMS mod. IM483) is 400 steps/rev.

Table 1 Characteristics of the step motor tested.

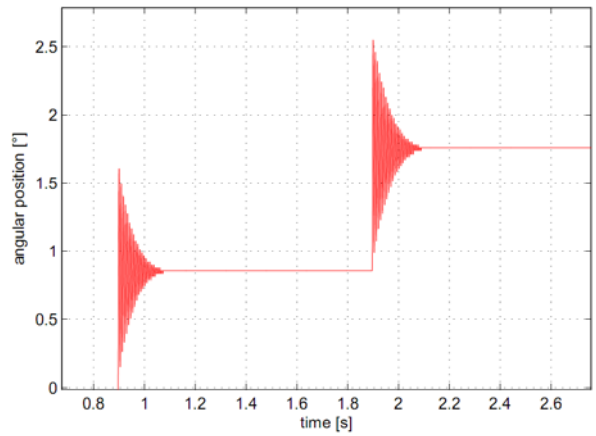
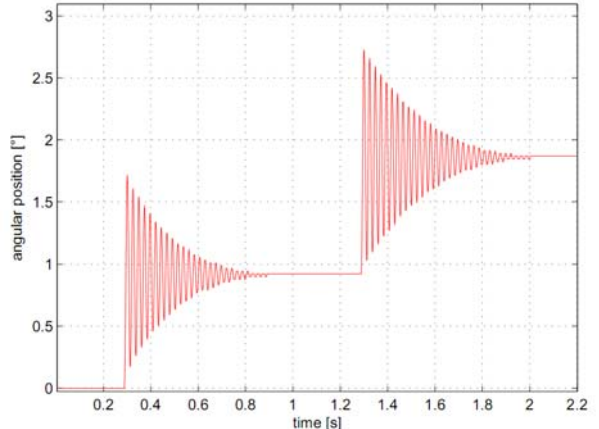
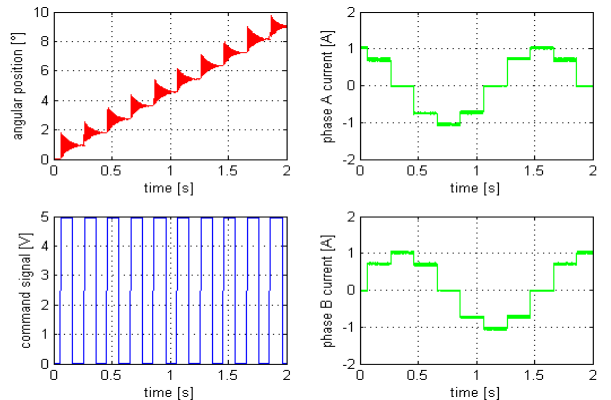
Size (mm)	Step angle ($^{\circ}$)	Nominal phase current (A)	Phase resistance (Ohm)	Phase inductance (mH)	Holding torque (Ncm)	Rotor's moment of inertia (kgm^2)	Back electromotive force (V/krpm)
42	1.8	0.7	3.15	3	25	43e-7	14

**Fig. 11** $f_c = 1 \text{ Hz}$, $n_p = 400 \text{ steps/rev}$, $J = J_1$.

should be noted that the phase currents' graphs have the typical shape of a half-step resolution: When the rotor is in the middle of the motor's step angle (1.8°), the phases are both supplied. Moreover, it's evident from Fig. 11 that the drive has an inner current closed loop; as a matter of fact, the phase current is kept constant for the whole supply interval.

Thanks to the high resolution encoder, the rotor's oscillation inside the step can be accurately measured. The graph of Fig. 12 highlights the rotor's angular position, and it clearly shows the shaft's oscillatory behaviour. Fig. 13 shows the decrease of the oscillation frequency, as the shaft's moment of inertia increases ($J = J_2$). Figs. 14-15 deal with tests carried-on with the same command frequency (5 Hz), the same shaft's moment of inertia (J_1) but different resolutions, 400 and 800 steps/rev. It's clear from the graphs that the same angular displacement is achieved with a different number of steps (double for $n_p = 800 \text{ steps/rev}$); moreover, at 800 steps/rev, the phases currents vary on nine levels rather than five levels, as for the half step resolution.

As already mentioned in the previous section, there are some running conditions when the step motor's shaft loses the synchronism with the magnetic field,

**Fig. 12** Rotor's oscillation highlight.**Fig. 13** Shaft's oscillation with $f_c = 1 \text{ Hz}$, $n_p = 400 \text{ steps/rev}$, $J = J_2$.**Fig. 14** $f_c = 5 \text{ Hz}$, $n_p = 400 \text{ steps/rev}$, $J = J_1$.

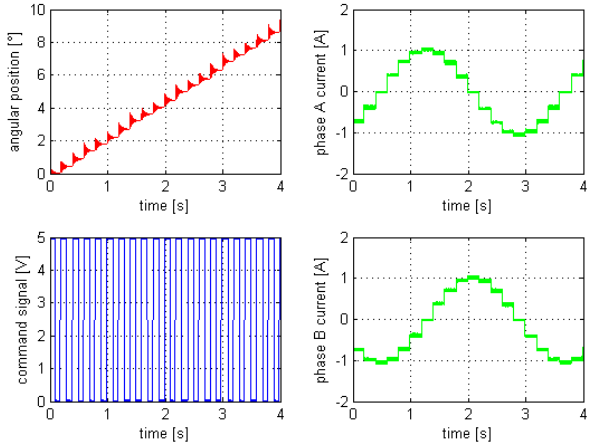


Fig. 15 $f_c = 5 \text{ Hz}$, $n_p = 800 \text{ steps/rev}$, $J = J_1$.

due to the phases' commutation. As an example, Fig. 16 shows the synchronism loss of the step motor under test for $f_c = 37 \text{ Hz}$, $n_p = 400 \text{ steps/rev}$, $J = J_2$. It is interesting to note that it's just a motor's problem, not a drive's one; as a matter of fact, the currents' graphs show that the phases are properly supplied, but the motor is not able to have a regular running.

When the command frequency increases, the rotor's motion becomes more regular; e.g., Figs. 17-18 show the motor's behaviour for $f_c = 100 \text{ Hz}$, and $f_c = 500 \text{ Hz}$. At the first command frequency, the motion becomes more regular, while at the second one the shaft does not oscillate any more.

In addition to low command frequency running, tests have been carried-on at high frequency too, in order to highlight the synchronism loss due to pull-out torque overcoming.

Fig. 19 shows the behaviour of the current in motor's phase A for increasing command frequencies ($n_p = 400 \text{ steps/rev}$, $J = J_2$). It should be noted that as the frequency increases, the phase current's shape changes: It has less and less time to keep its constant value.

Moreover, for high command frequencies, the current decreases leading to a decrease of the motor's torque that becomes not enough to guarantee regular running conditions.

This phenomenon is shown in Fig. 20, where the result of a sweep test is represented. The motor has been commanded by a 10 s long sine sweep with a

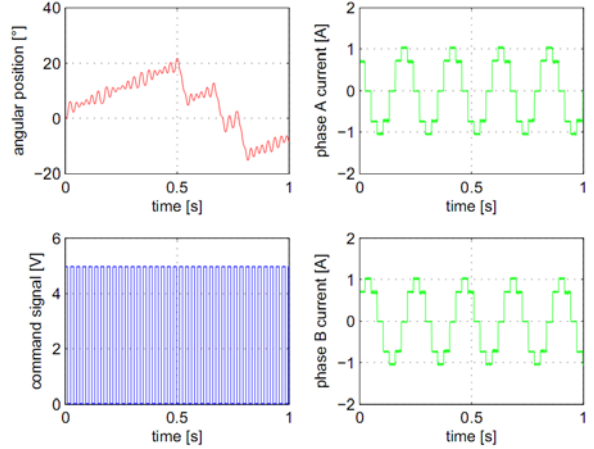


Fig. 16 Synchronism loss.

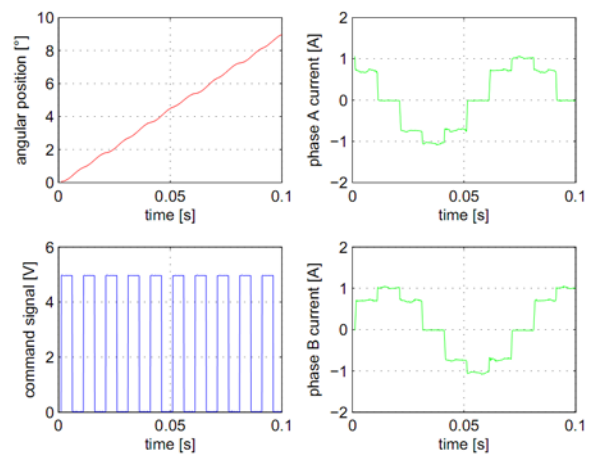


Fig. 17 Command frequency 100 Hz.

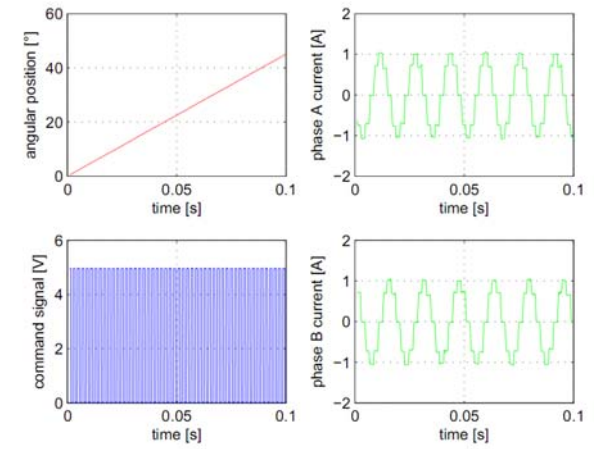


Fig. 18 Command frequency 500 Hz.

starting frequency of 2000 Hz and a stop frequency of 2300 Hz. For a command frequency of about 2100 Hz, the rotor loses synchronism and stops: The pull-out limit has been reached.

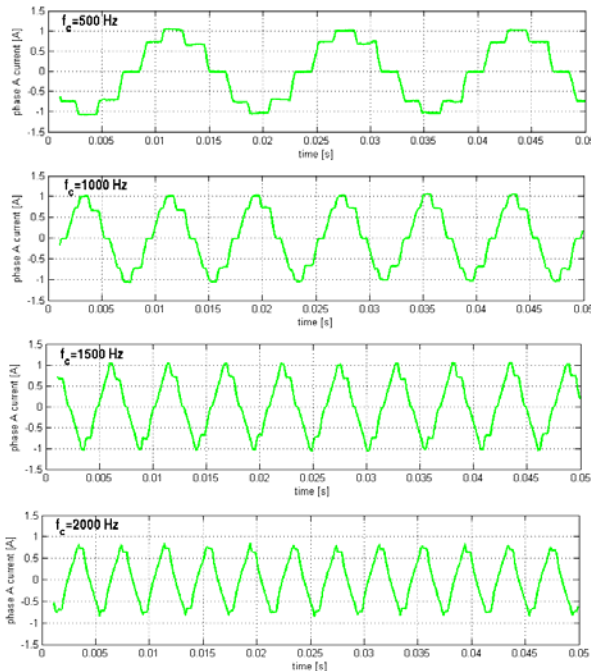


Fig. 19 Behavior of a phase current for increasing command frequency.

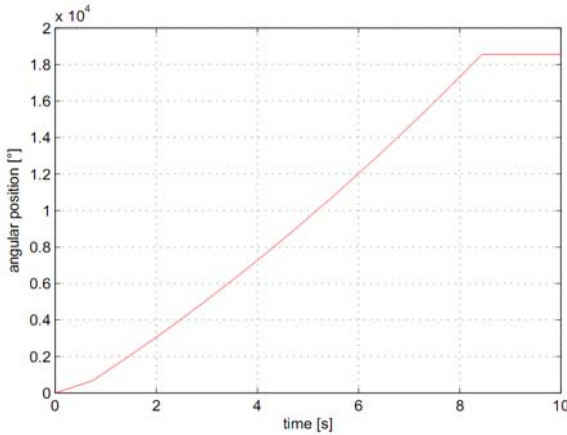


Fig. 20 Sweep test $f_c = 2000/3000 \text{ Hz}$.

Another sweep test has been carried-on at low frequencies, a 10 s sweep between 1 and 50 Hz. The results of such a test are summarized in Fig. 21 where the black circle highlights the crossing of a synchronism loss zone, as already mentioned before and shown in Fig. 16.

5. Results Discussion

From the analysis of these preliminary tests, some remarks can be made. A first comment concerns the resonance frequency of the step motor; by calculating

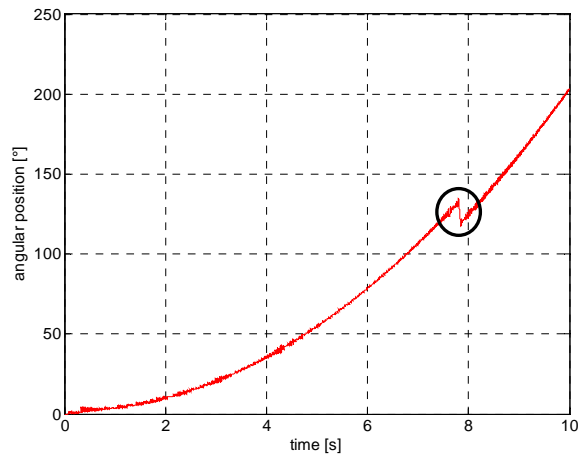


Fig. 21 Sweep test $f_c = 1/50 \text{ Hz}$.

that frequency from Eq. (4) for the J_1 moment of inertia, 123.97 Hz is obtained. The comparison between this value and the frequencies got from the measures, for different command frequencies and different motor's resolutions, leads to the results summarized in Tables 2-3, where also the viscous damping factor is highlighted.

As evidenced by the values of Tables 2-3, they are very similar to the natural frequency calculated, even if in Eq. (4) the holding torque T_H is used without taking into account the dependence of the motor's torque on the command frequency (i.e., the pull-out curve is not considered).

Moreover, the oscillatory behavior of the motor's shaft is well modeled by Eq. (3), where the damping factor calculated from the experimental results is used. Figs. 22-23 show the comparison between experimental and simulation results.

Another interesting remark arising from experimental results analysis is the dependence of the calculated viscous damping factor on the command frequency. As shown in Tables 2-3, the percentage variation of the damping factor is quite significant.

As a matter of fact, one of the aims of the experimental activity is just the investigation on the viscous damping factor of a step motor and its links with the running conditions.

During the development of these experimental tests, some command frequency ranges causing bad running

Table 2 Natural frequencies and viscous damping factors for $n_p = 400$.

f_c (Hz)	f_n (Hz)	ζ
1	121.98	0.0203
5	123.47	0.0189
10	125.03	0.0205
50	119.12	0.0349

Table 3 Natural frequencies and viscous damping factors for $n_p = 800$.

f_c (Hz)	f_n (Hz)	ζ
1	123.52	0.0324
5	121.96	0.0151
10	122.01	0.0298
50	123.55	0.0396

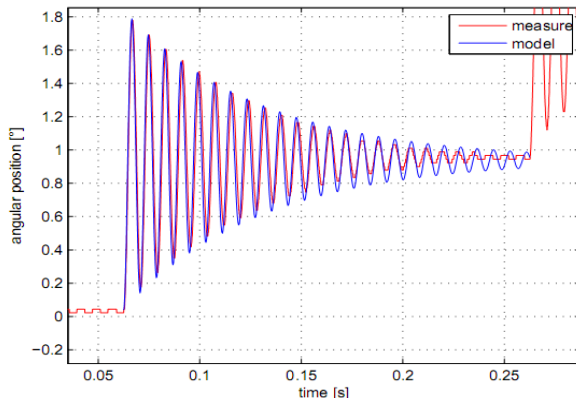


Fig. 22 Experimental vs. model results: $f_c = 5$ Hz, $n_p = 400$ steps/rev, $J = J_1$.

conditions have been highlighted. These ranges are related to the motor's natural frequency. As an example, Fig. 24 shows the measures for a range around 37 Hz.

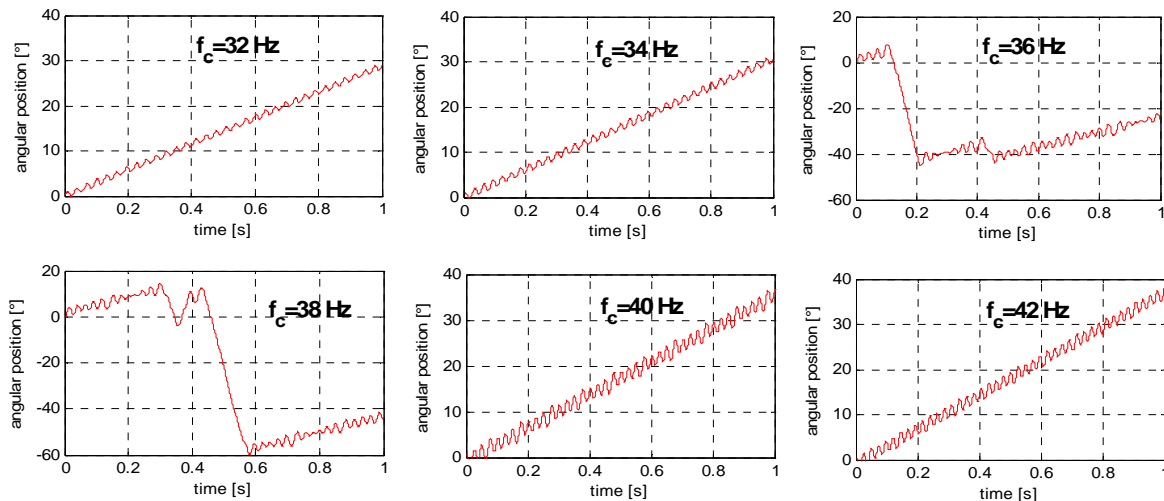


Fig. 24 Range where bad running conditions arise ($n_p = 400$ steps/rev, $J = J_1$).

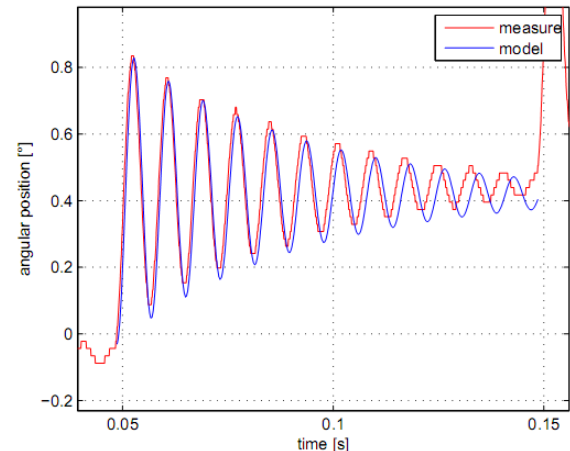


Fig. 23 Experimental vs. model results: $f_c = 10$ Hz, $n_p = 800$ steps/rev, $J = J_1$.

6. Conclusions

Within the present work, a test bench for the experimental analysis of the dynamic behaviour of step motors has been designed and developed.

Objective of the bench is to measure either mechanical or electrical quantities characterizing small size step motors with holding torque lower than 2 Nm. Hence, the experimental set-up has an encoder for motor's angular position measurement, a torque sensor and current sensors.

Moreover, the system can be configured in two different ways according to the kind of test: pull-out configuration, in order to measure the pull-out curve; inside-step configuration, in order to investigate the oscillatory behaviour of the motor.

Within this work, preliminary tests in the inside-step configuration have been carried-on; these tests have shown that the bench is suitable to properly investigate the dynamic behaviour of step motors. The preliminary tests carried on have also allowed to highlight some interesting aspects concerning the natural frequencies and the viscous damping factors.

In future works, tests in pull-out configuration will be carried-on, in order to completely validate the test bench.

Moreover, this test bench is the starting point for a large series of experimental tests devoted to validate the step motor's models and identify their unknown parameters.

References

- [1] T. Kenjo, Stepping Motors and Their Microprocessor Controls, Clarendon Press, Oxford, 1985.
- [2] L. Cao, H.M. Schwartz, Oscillation, instability and control of stepper motors, Nonlinear Dynamics 18 (1999) 383-404.
- [3] A.M. Harb, A.A. Zaher, Nonlinear control of permanent magnet stepper motors, Communications in Nonlinear Science and Numerical Simulation 9 (2004) 443-458.
- [4] J.R. Rogers, K. Craig, On-hardware optimization of stepper-motor system dynamics, Mechatronics 15 (2005) 291-316.
- [5] F. Nollet, T. Floque, W. Perruquetti, Observer-based second order sliding mode control laws for stepper motors, Control Engineering Practice 16 (2008) 429-443.
- [6] M. York, Model of a stepper motor for dynamic simulation, in: 5th Summer School on Mechanics of IUTAM, Aalborg University, Denmark, 1994.
- [7] P. Righettini, R. Strada, V. Lorenzi, B. Zappa, Modelling and dynamic simulation of mechanical systems driven by stepper motors, in: 11th International Conference on Power Electronics and Motion Control EPE-PEMC, Riga, Latvia, 2004.
- [8] V. Lorenzi, P. Righettini, R. Strada, B. Zappa, Analysis of the mechanical characteristics of stepper motor drives: Design of an experimental test bench, in: 7th International Workshop on Research and Education in Mechatronics, Stockholm, Sweden, 2006.